A Prototype Dual-Feedback CPM Device: Precision ROM and EMG Integration for Knee Rehabilitation

Ploypailin Rakthum
Department of Mechatronics Engineering, Rajamangala University of Technology Thanyaburi, Thailand
ploypailin_r@mail.rmutt.ac.th

Dechrit Maneetham
Department of Mechatronics Engineering, Rajamangala University of Technology Thanyaburi, Thailand
dechrit_m@rmutt.ac.th (corresponding author)

Myo Min Aung
Department of Mechatronics Engineering, Rajamangala University of Technology Thanyaburi, Thailand
myomin_a@rmutt.ac.th

Tenzin Rabgyal
Asian Institute of Technology, Thailand
tenzin@ait.ac.th

Received: 17 November 2025 | Revised: 21 December 2025 | Accepted: 29 December 2025

 DOI: https://doi.org/10.48084/etasr.16338

ABSTRACT

Existing knee Continuous Passive Motion (CPM) devices lack physiological feedback, and therefore cannot verify whether muscles are actively engaged during rehabilitation. This study presents a dual-feedback knee CPM device that integrates precise Range of Motion (ROM) control with real-time muscle activity monitoring. Encoder feedback enables closed-loop ROM control from 22° to 90°, with adjustable movement speeds from 0.64°/s to 4.39°/s, achieving high positional accuracy (Root Mean Square Error (RMSE) 0.0303–0.5802°) across repeated cycles. Surface Electromyography (EMG) measurements of the Rectus Femoris (RF) capture muscle activity, showing low activation during extension (EMG values of 50–150) and increased activation during flexion (EMG values of 250–350). The synchronized ROM and EMG signals confirm a temporal correlation between joint motion and muscle response, demonstrating that the system can quantify both positioning accuracy and muscle activation behavior during CPM-assisted movement. The integration of ROM precision and EMG monitoring forms a novel dual-feedback architecture for knee CPM rehabilitation, enabling objective and data-driven evaluation rather than subjective observation.

Keywords-CPM; EMG; encoder; microcontroller; knee rehabilitation

I. INTRODUCTION

Rehabilitation of patients recovering from musculoskeletal injuries, particularly knee disorders, remains a critical challenge in modern healthcare. Knee injuries arising from aging, athletic activities, and road accidents are highly prevalent and frequently lead to reduced mobility, stiffness, and impaired quality of life [1]. Total knee arthroplasty and other postoperative procedures require long-term rehabilitation to restore joint function and reduce complications. Continuous Passive Motion (CPM) therapy has therefore become an essential component of postoperative and musculoskeletal rehabilitation programs. By delivering repetitive and precisely controlled flexion-extension movements for the knee, CPM devices promote synovial fluid circulation, reduce joint swelling, and facilitate early restoration of Range of Motion (ROM) [2]. Normative studies report that healthy adult knees achieve passive flexion of approximately 140-150° and full extension of 1-5° [3]. However, in symptomatic or postoperative knees, the flexion is 70-90° immediately after surgery [4]. Figure 1 illustrates the typical ROM of the human knee.

Recent developments in rehabilitation engineering have aimed at enhancing CPM devices by integrating actuation control, adding sensors and feedback. Early CPM devices were

mechanically designed for fixed angular trajectories and uniform motor velocities that could not easily be modified according to specific patient recovery. To overcome these limitations, some studies developed controllable ROM and velocity to enhance comfort and avoid overstretch during rehabilitation [5, 6]. Hybrid rehabilitation mechanisms, combining passive and active training scenarios, have also been investigated to enhance therapy flexibility and patient interaction [7].

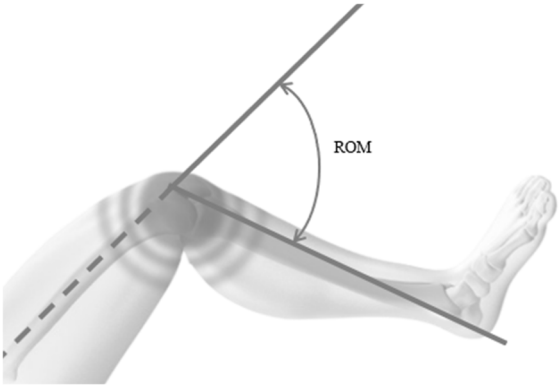

Fig. 1. Typical ROM of the human knee.

Several studies have introduced kinematic feedback using rotary encoders, potentiometers, or inertial sensors to enhance the motion accuracy and reliability (track ROM in real-time and verify the trajectory) [8]. In addition, closed-loop control methodologies such as Proportional–Integral–Derivative (PID) control [9], adaptive control, and model-based algorithms have been used to obtain smooth motion profiles and improved positioning accuracy [10, 11]. Although these methods improve the motion control to a great extent, they mostly depend on kinematic data and lack consideration of physiological responses from the patient during rehabilitation.

Surface Electromyography (EMG) has also been widely studied as a method for tracking muscle activity, fatigue, and neuromuscular recovery in rehabilitation settings [12, 13]. Rehabilitation and robotic systems that utilize EMG have shown the capacity to adjust movement based on muscle activation through the use of intelligent control methods, including fuzzy logic approaches [14]. Nevertheless, the majority of EMG-based systems are developed for active or assistive rehabilitation devices instead of CPM systems, and EMG is frequently employed for evaluation purposes rather than being incorporated into the motion control system. The integration of kinematic feedback and physiological sensing in the knee CPM devices is currently not documented in existing research.

As a response to this research gap, this study describes a dual-feedback CPM system combining encoder-based kinematic sensing with surface EMG monitoring for joint motion and muscular response measurement concurrently during passive rehabilitation. The proposed system has been integrated with an ESP32-controlled slider–crank mechanism, where adjustable motion parameters along with data acquisition capabilities are possible. The core value of this work is that it combines precise motion tracking and real-time EMG monitoring in a single passive-motion CPM framework, enhancing safety, personalization, and suitability for rehabilitation applications.

II. MATERIALS AND METHODS

The methodology describes the design and validation of the CPM device with EMG monitoring, covering hardware architecture, kinematic modeling, control and sensor modules.

A. Hardware

The primary hardware component of a CPM device for knee rehabilitation is the motorized mechanism, which enables controlled and repetitive movement of the knee joint. A DC motor coupled with a lead screw assembly provides the necessary torque to replicate the knee's natural kinematics, allowing precise adjustments of motion range and speed according to the patient's rehabilitation needs.

1) Kinematic Mechanisms

The proposed structure of the CPM device is based on a slider–crank mechanism. In this configuration, Link 2 (L_2) functions as the driver link, which is connected to a lead screw and powered by a DC motor. The corresponding Free-Body Diagram (FBD) is presented in Figure 2.

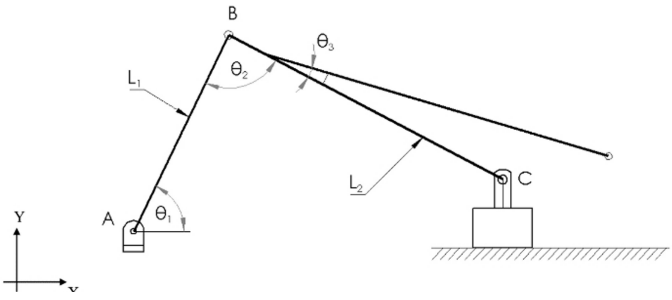

Fig. 2. FBD of the slider–crank mechanism.

The geometric positions of the points in the construction are defined within the Cartesian coordinate system (XY). The dimensional relationships of the links can be described by (1), (2), and (3), which provide a clear representation of the link dimensions in the system's geometry.

$$L_1^2 = X_B^2 + Y_B^2 \quad (1)$$

$$L_2^2 = (X_C - X_B)^2 + (Y_C - Y_B)^2 \quad (2)$$

Combining (1) and (2):

$$L_2^2 = \left(X_C - \sqrt{(L_1^2 - Y_B^2)}\right)^2 + (Y_C - Y_B)^2 \quad (3)$$

Rearranging (3) to solve for Y_B:

$$Y_B = \pm\sqrt{\left\{L_1^2 - \left(X_C \pm \sqrt{\{L_2^2 - (Y_C - Y_B)^2\}}\right)^2\right\}}$$

In this equation, there are two possible solutions for Y_B due to the presence of both a positive and a negative square root. However, considering the geometric constraints and the FBD, it is evident that the physically valid solution is the positive

value of Y_B. Thus, the value of Y_B is derived from the following equation:

$$Y_B = \sqrt{\left\{L_1^2 - \left(X_C - \sqrt{\{L_2^2 - (Y_C - Y_B)^2\}}\right)^2\right\}} \quad (4)$$

The following design constants were used: L_1 = 265 mm, L_2 = 375 mm, Y_C = 63 mm, and X_C varies between 410 and 610 mm, as detected by the encoder pulses.

After finding the coordinates of the mechanism's points, the dot product of two vectors is used to find θ_2, which is the angle between links 1 and 2:

$$L_1 \cdot L_2 \cdot cos(\theta_2) = \overrightarrow{BA} \times \overrightarrow{BC}$$

$$L_1 \cdot L_2 \cdot cos(\theta_2) = (X_A - X_B)(X_C - X_B) + (Y_A - Y_B)(Y_C - Y_B) \quad (5)$$

Point A is the origin coordinate (0,0).

$$\theta_2 = cos^{-1}\left(\frac{-X_B(X_C - X_B) - Y_B(Y_C - Y_B)}{L_1 \cdot L_2}\right) \quad (6)$$

From the FBD, the angle θ_3 is fixed at 11.2°. The total ROM of the mechanism is determined using the following equation:

$$\text{ROM} = 180 - (\theta_2 + \theta_3) \quad (7)$$

2) Driver System

The actuation system comprised a 12 V DC motor driven by a BTS7960 dual H-bridge module for precise bidirectional motion control. The BTS7960 accepted a Pulse-Width Modulation (PWM) command from the controller to regulate motor speed via duty-cycle modulation, whereas direction was set by H-bridge polarity reversal [15]. The motor's rotary output was coupled to a lead-screw transmission, which converted rotation into linear carriage travel. This linear motion actuated the limb support to deliver controlled knee flexion–extension, providing the torque capacity and velocity resolution required for CPM therapy within the experimental protocol, as shown in Figure 3.

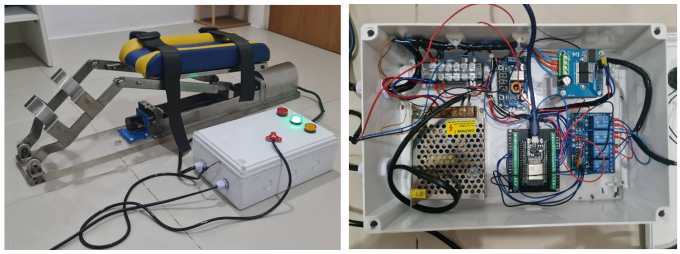

Fig. 3. CPM device for knee rehabilitation.

3) Control Unit

The ESP32 microcontroller serves as the control unit, providing general-purpose I/O and on-chip peripherals: PWM, Analog-to-Digital Converter (ADC), Inter-Integrated Circuit (I²C), Serial Peripheral Interface (SPI), and Universal Asynchronous Receiver/Transmitter (UART) for interfacing with sensors and actuators. In this design, the ESP32 is programmed in C++ using the Arduino framework; it generates PWM for speed control and logic-level direction commands to the BTS7960 motor driver, and it reads encoder counts, EMG signals, and limit-switch inputs for feedback and safety. Figure 4 shows a block diagram of the electronic components for the CPM device.

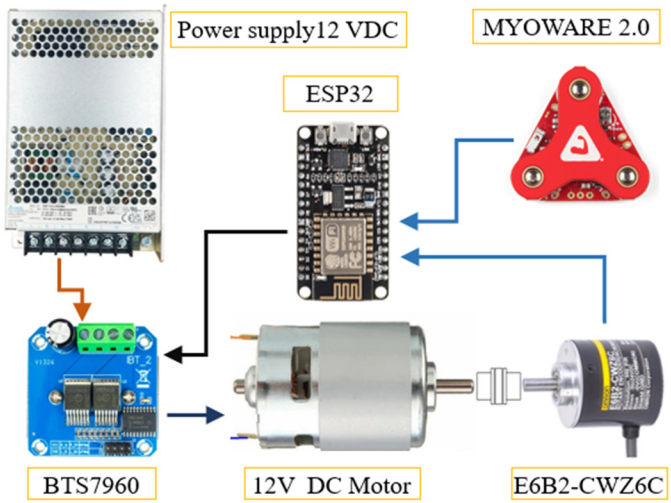

Fig. 4. Block diagram of the electronic components for the CPM device.

4) Motion Sensor

An E6B2-CWZ6C rotary encoder is used to monitor knee movement. Mounted at the end of the lead screw (via a shaft coupling), it converts rotation into digital pulses that the ESP32 counts and translates into angular displacement. This principle enables accurate measurement of flexion and extension angles during CPM operation.

5) Muscle Sensor

During rehabilitation, the EMG sensor (MyoWare 2.0) is used to verify proper muscle response by continuously monitoring electrical activity in the target muscle. Under normal conditions, skeletal muscles produce minimal electrical activity at rest; however, during knee movement, EMG detects and records the muscle's electrical signals [16, 17], confirming that activation corresponds to the intended motion. This integration allows simultaneous assessment of muscle activity and joint kinematics, optimizing the rehabilitation process and facilitating early detection of abnormal muscle responses that may hinder recovery.

The EMG operates by detecting and recording the electrical potentials generated by muscle fibers when stimulated by motor neurons [18, 19]. The EMG value represents the raw ADC output (12-bit, 0–4095 range) obtained from the MyoWare 2.0 sensor. Electrode placement is a critical factor; electrodes detect the summed motor unit action potentials of the target muscle, and accurate placement minimizes crosstalk. Following the Surface Electromyography for Non-Invasive Assessment of Muscles (SENIAM) guideline for the Rectus Femoris (RF), the bipolar pair was positioned at 50% of the line between the Anterior Superior Iliac Spine (ASIS) and the superior border of the patella, aligned with the muscle fiber direction [20]. Skin preparation was performed as shown in

Figure 5. The RF was selected because it is a superficial, bi-articular component of the quadriceps responsible for knee extension, making it directly relevant for tracking muscle activation during flexion–extension movements in rehabilitation tasks.

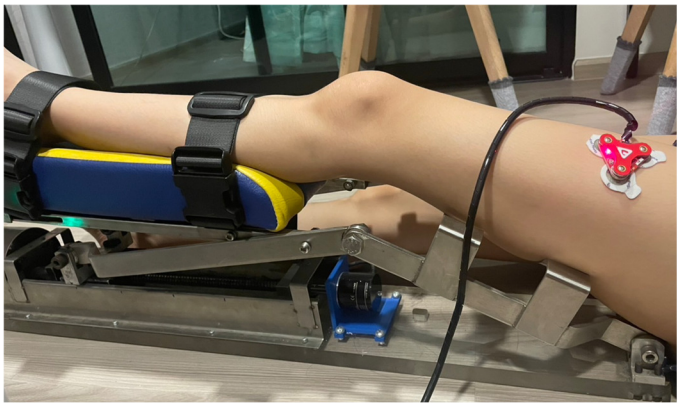

Fig. 5. EMG placement on the RF muscle.

B. System Flowchart

The system flowchart outlines the sequential operation of the prototype dual-feedback CPM device, integrating encoder-based kinematic measurement and EMG signal acquisition for precise motion control. The process begins with system initialization and homing to establish a reference position for accurate angle tracking. The control loop interprets user-defined or preset parameters to execute controlled flexion–extension cycles of the knee joint while synchronizing encoder and EMG feedback in real time. Once the preset cycles are completed, the device halts and returns to the home position, ensuring repeatable movement and reliable physiological data for rehabilitation assessment, as shown in Figure 6.

III. EXPERIMENT AND RESULTS

To validate the performance of the proposed CPM device, the system used an ESP32 controller driving a DC motor/lead-screw transmission with encoder-based angle tracking and surface EMG electrodes placed on the RF. Testing included a manual mode, in which the PWM duty cycle was stepped across predefined levels and angle setpoints to characterize speed control across different joint positions, and an automatic mode, where the device executed five continuous flexion–extension cycles between 22° and 90° at 100% PWM. This design allowed simultaneous assessment of speed regulation and ROM performance.

A trial was conducted with one healthy participant to assess device functionality. Encoder pulses were converted to knee angle using (1)-(7), whereas EMG captured muscle activation and the PWM duty cycle was logged for correlation with motor response. Checkpoints at 22°, 52°, 73°, and 90° were used to compute Root Mean Square Error (RMSE), quantify ROM precision, examine cycle-to-cycle repeatability, and relate PWM duty cycle to joint velocity, providing an initial demonstration of safe operation, accurate angle tracking, and controlled kinematics suitable for rehabilitation.

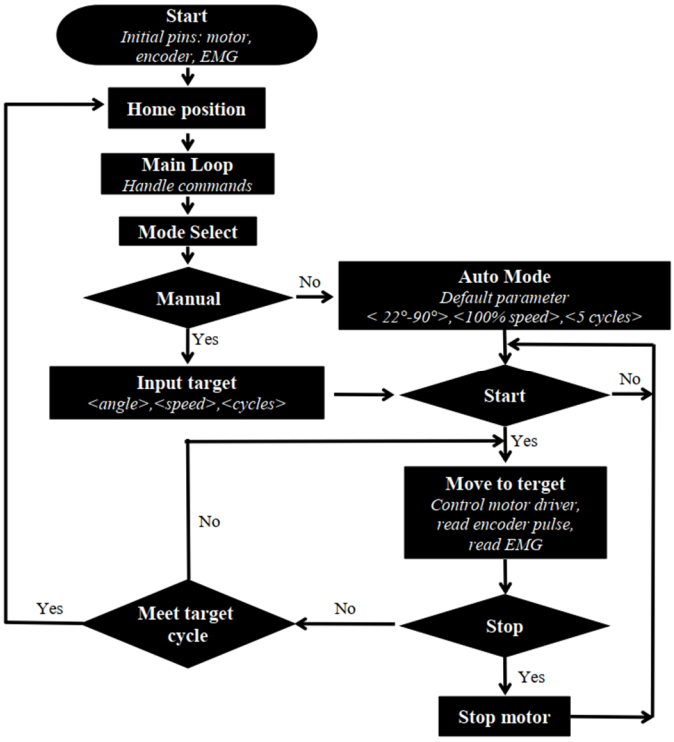

Fig. 6. System flowchart of the CPM device.

A. Accuracy of System Response

From Figure 7, tested at a target ROM of 52°, it can be observed that the angular velocity of the CPM device increases proportionally with the applied PWM percentage. This tunable speed response highlights the system's ability to adapt motion dynamics according to individual therapeutic requirements. At lower PWM levels (20–50%), the actuator generated slower and smoother movements, which are suitable for early-stage rehabilitation or patients with limited mobility. At 100% PWM, the device achieved a higher angular velocity, enabling faster ROM progression. As summarized in Table I, the measured rotation speed increased from 0.64°/s at 20% PWM to 4.39°/s at 100% PWM, confirming a nearly proportional relationship between speed and duty cycle. This adjustable speed profile is essential for minimizing injury risk while supporting gradual increases in movement intensity as recovery progresses, thereby enhancing rehabilitation effectiveness.

TABLE I. ROM SPEED AT DIFFERENT PWM

PWM (%)	Speed (°/s)
20	0.64
50	2.07
100	4.39

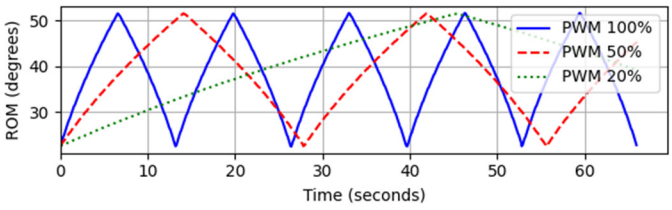

Fig. 7. Knee ROM at different PWM levels.

Figure 8 illustrates the ROM measured in three configurations using an encoder as a rotational position sensor. In manual mode, the system was tested at different target angles: 22°–52° ROM (Figure 8(a)) and 22°–73° ROM (Figure 8(b)), both operated at 100% PWM. in auto mode, the range was extended to 22°–90° ROM at the same PWM setting for five continuous cycles, as shown in Figure 8(c). The encoder continuously converts the motor's rotational motion into digital pulse counts, allowing the controller to calculate ROM in real time. When the system reaches the preset angle, the control algorithm reverses motor direction and repeats cyclically between defined limits. This closed-loop feedback mechanism ensures precise motion tracking of both flexion and extension movements and provides an automatic correction for minor deviations due to load variations or mechanical backlash. Consequently, the CPM device maintains consistent, repeatable trajectories across different target angles.

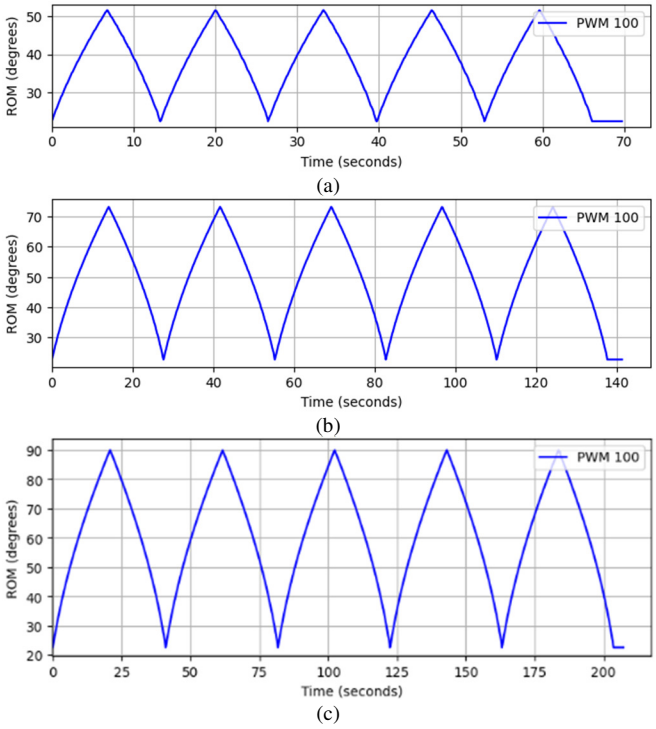

Fig. 8. Knee angle during manual and auto modes at 100% PWM: (a) manual mode 22°–52° ROM, (b) manual mode 22°–73° ROM, (c) auto mode 22°–90° ROM.

The measured joint angles and corresponding RMSE values are summarized in Table II. Across five consecutive cycles, the deviations from the target positions were minimal, with RMSE values of 0.5802° at the starting point, 0.4125° at 52°, 0.2163° at 73°, and 0.0303° at 90°. These results demonstrate that the system can reliably and precisely reproduce the programmed angular positions during both flexion and extension movements. The consistently low RMSE across all target angles confirms not only the high positional accuracy but also the mechanical stability and repeatability of the proposed CPM device.

TABLE II. KNEE ROM VALUES OVER FIVE CONSECUTIVE CYCLES

Cycle	Start point (22°)	Target 52°	Target 73°	Target 90°
1	22.61	51.60	73.22	90.04
2	22.57	51.57	73.26	89.98
3	22.57	51.62	73.23	89.99
4	22.58	51.58	73.19	90.05
5	22.57	51.57	73.17	90.00
RMSE	0.5802	0.4125	0.2163	0.0303

B. Muscle Activity Behavior

Figure 9 shows the EMG response of the RF muscle during passive ROM cycles at three target ROM levels (52°, 73°, and 90°). The ROM profile (blue trace) corresponds directly to the flexion–extension movement produced by the CPM device, whereas the EMG signal (red trace) represents the muscle activation occurring concurrently.

During the extension phase, when the limb is driven forward by the CPM device, the EMG amplitude remains low (EMG values 50–150). This indicates minimal voluntary muscle engagement, confirming that the device performs the motion passively and the patient is not required to activate the muscle. Conversely, during the flexion phase, the EMG amplitude increases substantially, typically ranging from 250–350, and peaks near the reversal point of each cycle. This consistent rise in activity indicates that flexion elicits greater neuromuscular involvement, even under passive CPM operation.

The distinction between low EMG activity during extension and pronounced activity during flexion indicates that the CPM device not only provides passive joint mobilization but also promotes beneficial muscle activation patterns. The integration of EMG feedback therefore confirms that the device supports rehabilitation by enabling therapists to monitor muscle engagement and adjust ROM or cycle parameters based on patient response.

IV. DISCUSSION

The proposed system does not present a new CPM mechanism or control theory but builds on existing DC motor motion control architectures that are prevalent in knee CPM systems. This study demonstrates motion-control capability in comparison with traditional knee CPM devices with embedded encoder feedback. Experimental results confirm high positional accuracy (RMSE < 0.6°) and consistent ROM performance.

In addition, this novel CPM system integrates surface EMG monitoring with kinematic sensing during passive motion. Unlike conventional knee CPM devices that assess rehabilitation through joint kinematics or EMG-driven active systems that rely on muscle activity, this system employs EMG exclusively for physiological monitoring. The observed EMG responses are consistent with muscle activity during passive knee motion, with low activity during extension and increased activation during flexion, providing additional insight into muscle response. This integrated kinematic-physiological framework improves traditional CPM evaluation by enabling simultaneous mechanical and physiological assessments.

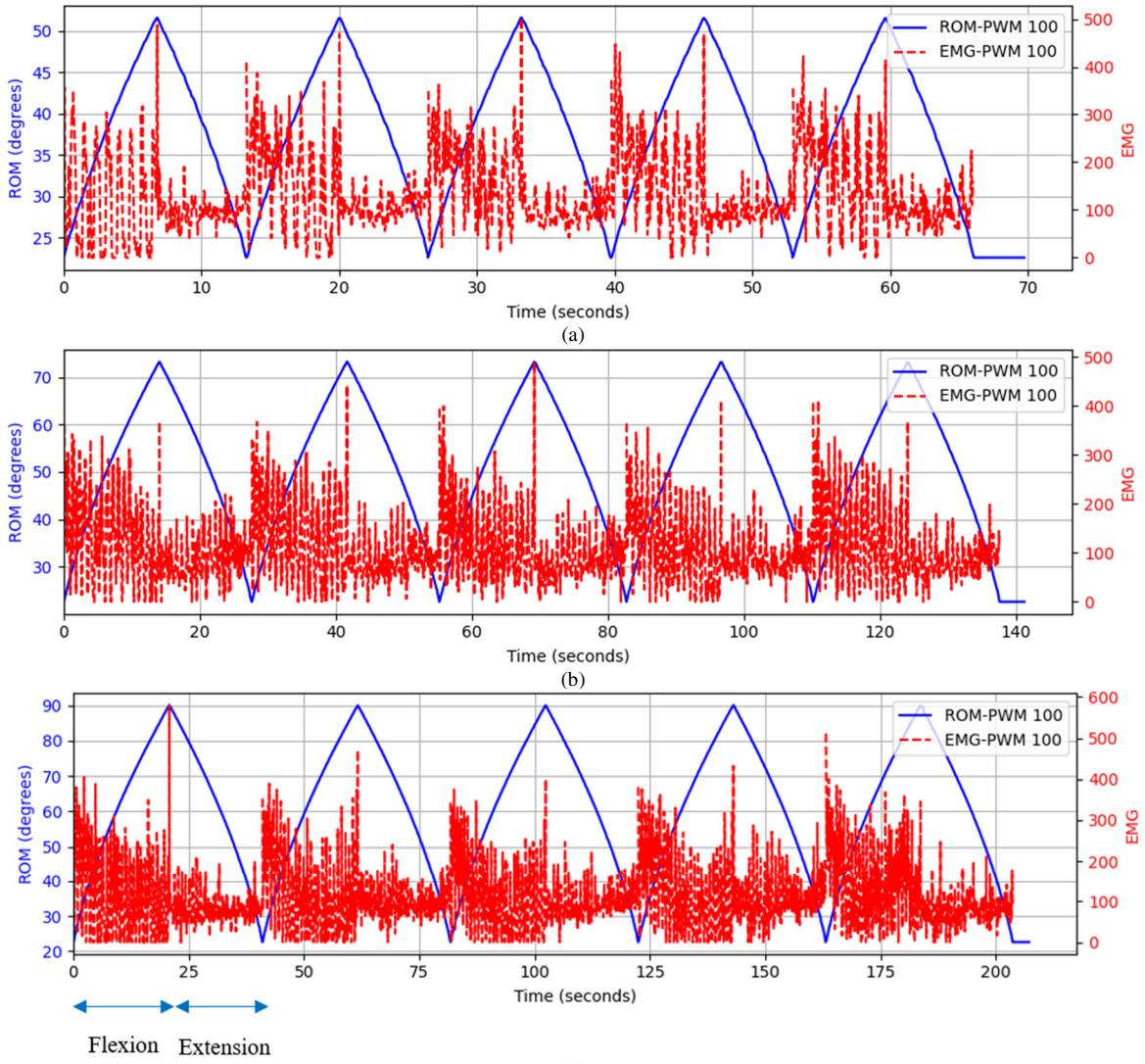

Fig. 9. EMG signal of the RF during CPM operation at 100% PWM: (a) 22°–52° ROM , (b) 22°–73° ROM , (c) 22°–90° ROM.

V. CONCLUSION

This work presented a prototype dual-feedback Continuous Passive Motion (CPM) device for knee rehabilitation. The system achieved a controllable Range of Motion (ROM) from 22° to 90° with adjustable movement speeds ranging from 0.64°/s (20% PWM) to 4.39°/s (100% PWM). Encoder feedback confirmed high positional accuracy across multiple cycles, demonstrating consistent and repeatable motion control. Surface Electromyography (EMG) measurements from the Rectus Femoris (RF) showed low activity during extension (EMG values 50–150) and increased activity during flexion (EMG values 250–350), verifying the correct synchronization between joint movement and muscle activation.

The novelty of this work lies in the integration of dual-feedback ROM position sensing and EMG monitoring within a single CPM system, enabling real-time evaluation of both mechanical motion and muscle activity. This dual-feedback approach addresses the limitations of conventional CPM devices, which lack physiological insight and cannot quantify patient involvement. Future work will focus on implementing adaptive control algorithms, expanding to multi-joint configurations, and conducting clinical validation.

REFERENCES

[1] Z. Khired *et al.*, "Knee pain and its influence on quality of life and physical function in Jazan adult population: A cross sectional study," *Clinical Epidemiology and Global Health*, vol. 22, July 2023, Art. no. 101346, https://doi.org/10.1016/j.cegh.2023.101346.

[2] B. C. Lee *et al.*, "Clinical evaluation of usefulness and effectiveness of sitting-type continuous passive motion machines in patients with total knee arthroplasty: a dual-center randomized controlled trial," *BMC Musculoskeletal Disorders*, vol. 25, no. 1, Dec. 2024, Art. no. 1039, https://doi.org/10.1186/s12891-024-08062-0.

[3] J. M. Soucie *et al.*, "Range of motion measurements: reference values and a database for comparison studies," *Haemophilia*, vol. 17, no. 3, pp. 500–507, May 2011, https://doi.org/10.1111/j.1365-2516.2010.02399.x.

[4] A. J. Kittelson *et al.*, "Reference chart for knee flexion following total knee arthroplasty: a novel tool for monitoring postoperative recovery," *BMC Musculoskeletal Disorders*, vol. 21, no. 1, July 2020, Art. no. 482, https://doi.org/10.1186/s12891-020-03493-x.

[5] S. Tangjitsitcharoen and H. Lohasiriwat, "Redesign of a continuous passive motion machine for total knee replacement therapy," *Journal of Health Research*, vol. 33, no. 2, pp. 106–118, Mar. 2019, https://doi.org/10.1108/JHR-06-2018-0024.

[6] M. Tagami, M. Hasegawa, W. Tanahara, and Y. Tagawa, "Prototype of a Continuous Passive Motion Device for the Knee Joint with a Function of Active Exercise," *Journal of Robotics and Mechatronics*, vol. 34, no. 1, pp. 28–39, Feb. 2022, https://doi.org/10.20965/jrm.2022.p0028.

[7] M. Tagami and Y. Tagawa, "Development of a continuous-passive-motion device with an active training mode for muscle recovery," in *2017 11th Asian Control Conference*, Gold Coast, Australia, 2017, pp. 2226–2231, https://doi.org/10.1109/ASCC.2017.8287521.

[8] R. Trochimczuk and T. Kuźmierowski, "Kinematic Analysis of Cpm Machine Supporting to Rehabilitation Process after Surgical Knee Arthroscopy and Arthroplasty," *International Journal of Applied Mechanics and Engineering*, vol. 19, no. 4, pp. 841–848, Nov. 2014, https://doi.org/10.2478/ijame-2014-0059.

[9] D. Maneetham and P. Sutyasadi, "Controlling a knee CPM machine using PID and iterative learning control algorithm," *TELKOMNIKA (Telecommunication Computing Electronics and Control)*, vol. 18, no. 2, pp. 1047–1053, Apr. 2020, https://doi.org/10.12928/telkomnika.v18i2.14876.

[10] C. H. Guzmán, A. Blanco, J. A. Brizuela, and F. A. Gómez, "Robust control of a hip–joint rehabilitation robot," *Biomedical Signal Processing and Control*, vol. 35, pp. 100–109, May 2017, https://doi.org/10.1016/j.bspc.2017.03.002.

[11] N.-B. Le, H.-N. Nguyen, D.-A. Nguyen, and H.-D. Vo, "Study on Mechanical Adaptive Design, Construction and Control of Knee Continuous Passive Motion Machine," *Journal of Automation and Control Engineering*, vol. 1, no. 3, pp. 227–231, Sept. 2013, https://doi.org/10.12720/joace.1.3.227-231.

[12] V. Bandini *et al.*, "Surface-Electromyography-Based Co-Contraction Index for Monitoring Upper Limb Improvements in Post-Stroke Rehabilitation: A Pilot Randomized Controlled Trial Secondary Analysis," *Sensors*, vol. 23, no. 17, Sept. 2023, Art. no. 7320, https://doi.org/10.3390/s23177320.

[13] R. Jastania, P. Wang, B. Alqahtani, A. Alzahrani, and W. Wang, "The Development of an Interface Instrument for Collecting Electromyography Data and Controlling a Continuous Passive Motion Machine," *Applied Sciences*, vol. 13, no. 22, Nov. 2023, Art. no. 12221, https://doi.org/10.3390/app132212221.

[14] N.-K. Nguyen, T.-M.-P. Dao, T.-D. Nguyen, D.-T. Nguyen, H.-T. Nguyen, and V.-K. Nguyen, "An sEMG Signal-based Robotic Arm for Rehabilitation applying Fuzzy Logic," *Engineering, Technology & Applied Science Research*, vol. 14, no. 3, pp. 14287–14294, June 2024, https://doi.org/10.48084/etasr.7146.

[15] K. M. Raza, Mohd. Kamil, and P. Kumar, "Speed Control of DC Motor by using PWM," *International Journal of Advanced Research in Computer and Communication Engineering*, vol. 5, no. 4, pp. 307–309, Apr. 2016, https://doi.org/10.17148/IJARCCE.2016.5478.

[16] A. J. Pesola, Y. Gao, and T. Finni, "Responsiveness of electromyographically assessed skeletal muscle inactivity: methodological exploration and implications for health benefits," *Scientific Reports*, vol. 12, no. 1, Dec. 2022, Art. no. 20867, https://doi.org/10.1038/s41598-022-25128-y.

[17] L. McManus, G. De Vito, and M. M. Lowery, "Analysis and Biophysics of Surface EMG for Physiotherapists and Kinesiologists: Toward a Common Language With Rehabilitation Engineers," *Frontiers in Neurology*, vol. 11, Oct. 2020, Art. no. 576729, https://doi.org/10.3389/fneur.2020.576729.

[18] M. Al-Ayyad, H. A. Owida, R. De Fazio, B. Al-Naami, and P. Visconti, "Electromyography Monitoring Systems in Rehabilitation: A Review of Clinical Applications, Wearable Devices and Signal Acquisition Methodologies," *Electronics*, vol. 12, no. 7, Apr. 2023, Art. no. 1520, https://doi.org/10.3390/electronics12071520.

[19] M. B. I. Reaz, M. S. Hussain, and F. Mohd-Yasin, "Techniques of EMG signal analysis: detection, processing, classification and applications," *Biological Procedures Online*, vol. 8, no. 1, pp. 11–35, Dec. 2006, https://doi.org/10.1251/bpo115.

[20] "Recommendations for Sensor Locations in Hip or Upper Leg Muscles—Quadriceps Femoris (Rectus Femoris)." Seniam. https://seniam.org/quadricepsfemorisrectusfemoris.html.